Laser Magnetic Resonance of the O_2 Molecule Using 119- and 78-μm H_2O Laser Lines*

K. M. Evenson
National Bureau of Standards, Quantum Electronics Division, Boulder, Colorado 80302

and

Masataka Mizushima
Department of Physics and Astrophysics, University of Colorado, Boulder, Colorado 80302
(Received 2 March 1972)

Laser magnetic resonance of the O_2 molecule is observed using the 119- and 78-μm lines of the H_2O laser. The relevant transitions for the 119-μm line are ($N=13$, $J=14, M$) $\rightarrow$ ($N=15$, $J=14$, M'), and those for the 78-μm line are ($N=21$, $J=22$, M) $\rightarrow$ ($N=23$, $J=22$, M'), where $M'=M$ or $M\pm1$ depending on the polarization. It is found that $g_\perp=2.0044\pm0.0008$, $g_z=2.0020\pm0.0001$, $g_n=0.000125\pm0.000008$ give slightly better agreement between theory and experiment than Hendrie and Kusch's values ($g_\perp=2.005169$, $g_z=2.001939$, $g_n=0.000122$) and Bauer, Kamper, and Lustig's values ($g_\perp=2.004838$, $g_z=2.002025$, $g_n=0.000126$), but the present experimental accuracy is not high enough to exclude these older g-factor values. Using the existing microwave data and the known laser frequencies, the zero-field frequencies for the transitions ($N=J=13$) $\rightarrow$ ($N=J=15$) and ($N=J=21$) $\rightarrow$ ($N=J=23$) are found to be 2496.283 ± 0.30 and 3865.81 ± 0.03 GHz, respectively. Combining these results with the frequency of the ($N=J=1$) $\rightarrow$ ($N=J=3$) transition obtained by McKnight and Gordy, we obtain $B_0=43.100518\pm0.000020$ GHz, $B_1=-0.14496\pm0.00030$ MHz, and $B_2=-0.17\pm1.00$ Hz.

I. INTRODUCTION

Each rotational level of the oxygen molecule O_2 in its ground electronic state ($^3\Sigma_g^-$) is a triplet. The rotational part of the Hamiltonian is

$$\hat{H}=B\vec{\mathrm{N}}^2+\tfrac{2}{3}\lambda(3S_z^2-\vec{\mathrm{S}}^2)+\mu\vec{\mathrm{N}}\cdot\vec{\mathrm{S}}\ , \tag{1}$$

where $\vec{\mathrm{N}}$ is the angular momentum of the end-over-end rotation, B is the rotational constant, $\vec{\mathrm{S}}$ is the spin angular momentum, μ is a coupling parameter, and $\vec{\mathrm{S}}_z$ is its component along the molecular axis. The middle term was introduced by Kramers[1] and Hebb,[2] and the last term was introduced by Schlapp.[3]

The transitions within each triplet have been observed in microwave spectroscopy.[4–10] Zimmerer and Mizushima[11] and West and Mizushima[12] remeasured these frequencies with high precision and refined the theory by taking into account the centrifugal stretching effects. McKnight and Gordy[13] observed $N=1\rightarrow3$ submillimeter transitions. Tischer[14] and Wilheit and Barrett[15] recalculated the values of the molecular parameters using existing theory and data.[11–13]

The 337-μm laser magnetic resonance of the $N=3\rightarrow5$ transition of this molecule was observed by Evenson, Broida, Wells, Mahler, and Mizushima[16] as the first application of this new technique.

II. MAGNETIC PERTURBATION

When an external magnetic field $\vec{\mathfrak{B}}$ is applied to the oxygen molecule the additional terms

$$\hat{H}_1=\mu_B g_\perp\vec{\mathrm{S}}\cdot\vec{\mathfrak{B}}+\mu_B(g_z-g_\perp)S_z\mathfrak{B}_z+\mu_B g_n\vec{\mathrm{N}}\cdot\vec{\mathfrak{B}} \tag{2}$$

appear in the Hamiltonian. Here μ_B is the Bohr magneton, 1.39961 MHz/G, g_z and $g_\perp$ are the parallel and perpendicular components of the electron spin g factor, and g_n is the g factor due to the end-over-end rotation.

The electron paramagnetic resonance (EPR) of this molecule was first observed by Beringer and Castle[17] and analyzed by Henry.[18] Tinkham and Strandberg[19] measured the resonance fields with high accuracy and analyzed their own data according to Eq. (2) but assumed that g_z is equal to the g factor of a free electron, 2.00232. Bauers, Kamper, and Lustig[20] and Tischer[14] remeasured the EPR fields and obtained

$$g_\perp=2.004838\pm0.000030,\quad g_z=2.002025\pm0.000020,\quad g_n=0.000126\pm0.000012\ . \tag{3a}$$

Their values are slightly different from the values obtained by Hendrie and Kusch[21] using the molecular-beam technique:

$$g_\perp=2.005169\pm0.000056,\quad g_z=2.001939\pm0.000026,\quad g_n=0.000122\pm0.000015\ . \tag{3b}$$

In order to calculate the perturbation due to $\hat{H}_1$ it is convenient to express the eigenfunctions of $\hat{H}$ as

$$|N_0M\rangle\cong|NNM\rangle\ , \tag{4a}$$

$$|N_-M\rangle\cong a_{N-1}|NN-1M\rangle+b_{N-1}|N-2N-1M\rangle\ , \tag{4b}$$

$$|N_+M\rangle\cong a_{N+1}|NN+1M\rangle-b_{N+1}|N+2N+1M\rangle\ , \tag{4c}$$

where, in each term on the right-hand side, $|NJM\rangle$ is an eigenfunction of $\hat{N}^2$, $\hat{S}^2$, $\hat{J}^2$, and $\hat{J}_z$ with appropriate eigenvalues. It is found that

$$\begin{array}{lcccccc} J= & 12 & 14 & 16 & 20 & 22 & 24\,, \\ a_J= & 0.99965 & 0.99970 & 0.99979 & 0.99987 & 0.99989 & 0.99990\,, \\ b_J= & 0.0265 & 0.0246 & 0.0203 & 0.0164 & 0.0150 & 0.0138\,. \end{array} \tag{5}$$

The matrix elements of $\hat{H}_1$ within each triplet are

$$\langle N_0 M|\hat{H}_1|N_0 M\rangle = \mathfrak{G}\mu_B M\left(\frac{g_z-g_n}{N(N+1)}+g_n\right), \tag{6a}$$

$$\langle N_- M|\hat{H}_1|N_- M\rangle = \mathfrak{G}\mu_B M\left\{-(g_\perp-g_n)\left(\frac{a_{N-1}^2}{N}-\frac{b_{N-1}^2}{N-1}\right)+\frac{g_z-g_\perp}{2N-1}\left[\frac{a_{N-1}^2}{N}+\frac{b_{N-1}^2}{N-1}+2a_{N-1}b_{N-1}\left(\frac{2N-3}{N(N-1)(2N+1)}\right)^{1/2}\right]+g_n\right\}, \tag{6b}$$

$$\langle N_+ M|\hat{H}_1|N_+ M\rangle = \mathfrak{G}\mu_B M\left\{(g_\perp-g_n)\left(\frac{a_{N+1}^2}{N+1}-\frac{b_{N+1}^2}{N+2}\right)+\frac{g_z-g_\perp}{2N+3}\left[\frac{a_{N+1}^2}{N+1}+\frac{b_{N+1}^2}{N+2}-2a_{N+1}b_{N+1}\left(\frac{2N+1}{(N+1)(N+2)(2N+5)}\right)^{1/2}\right]+g_n\right\}, \tag{6c}$$

$$\langle N_0 M|\hat{H}_1|N_- M\rangle = \mathfrak{G}\mu_B\left[a_{N-1}\left(g_\perp-g_n+(g_z-g_\perp)\frac{N-1}{2N-1}\right)+b_{N-1}(g_z-g_\perp)\frac{[N(N-1)]^{1/2}}{2N-1}\right]\frac{[(N^2-M^2)(N+1)]^{1/2}}{N(2N+1)^{1/2}}, \tag{6d}$$

$$\langle N_0 M|\hat{H}_1|N_+ M\rangle = \mathfrak{G}\mu_B\left[a_{N+1}\left(g_\perp-g_n+(g_z-g_\perp)\frac{N+2}{2N+3}\right)-b_{N+1}(g_z-g_\perp)\frac{[(N+1)(N+2)]^{1/2}}{2N+3}\right]\frac{\{[(N+1)^2-M^2]N\}^{1/2}}{(N+1)(2N+1)^{1/2}}, \tag{6e}$$

$$\langle N_- M|\hat{H}_1|N_+ M\rangle = 0\,. \tag{6f}$$

Since b_J and $g_z-g_\perp$ are both small, terms which contain $b_J(g_z-g_\perp)$ are negligible in our calculations.

Small contributions to the perturbation appear when the interaction between neighboring triplets is taken into account. The matrix elements of $\hat{H}_1$ between the triplet states with N and those with $N-2$ are

$$\langle N_0 M|\hat{H}_1|N-2_+ M\rangle = \mathfrak{G}\mu_B\left(a_{N-1}(g_z-g_\perp)\quad b_{N-1}(g_\perp-g_n)\frac{2N-1}{[N(N-1)]^{1/2}}\right)\left(\frac{(N-1)(N+1)(N^2-M^2)}{(2N-1)^2N(2N+1)}\right)^{1/2}, \tag{7a}$$

$$\langle N_- M|\hat{H}_1|N-2_0 M\rangle = \mathfrak{G}\mu_B\left(a_{N-1}(g_z-g_\perp)\quad b_{N-1}(g_\perp-g_n)\frac{2N-1}{[N(N-1)]^{1/2}}\right)\left(\frac{N(N-2)[(N-1)^2-M^2]}{(2N-1)^2(N-1)(2N-3)}\right)^{1/2}, \tag{7b}$$

$$\langle N_- M|\hat{H}_1|N-2_+ M\rangle = \mathfrak{G}\mu_B a_{N-1}\left[a_{N-1}(g_z-g_\perp)\frac{1}{2N-1}\left(\frac{2N-3}{N(N-1)(2N+1)}\right)^{1/2}-b_{N-1}(g_\perp-g_n)\frac{2N-1}{N(N-1)}\right]M, \tag{7c}$$

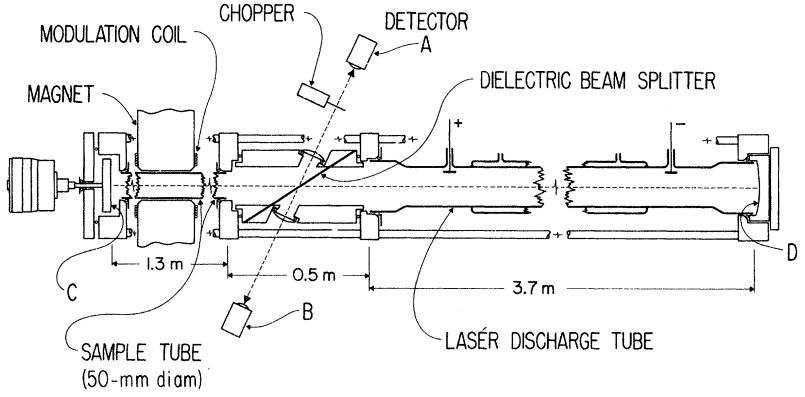

FIG. 1. Schematic diagram of the apparatus.

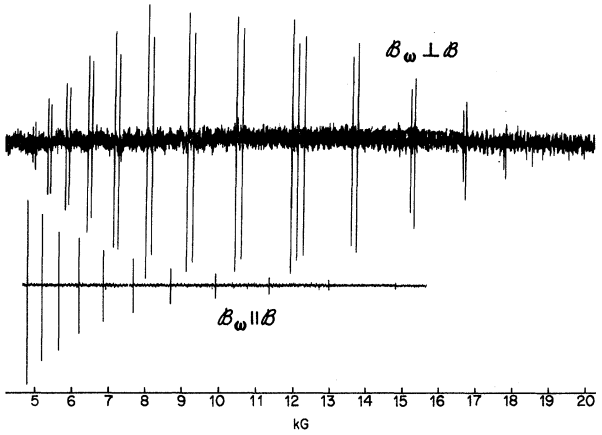

FIG. 2. Typical chart recorder traces of the laser magnetic resonance of the O_2 molecule using the 119-μm H_2O laser line. Tables I and II give the field strengths and assignments of the resonance lines in the lower and upper traces, respectively. One of the triplet lines near the center of the upper trace is unexplained. $\mathcal{B}$ is the external magnetic field, while $\mathcal{B}_\omega$ gives the direction of the magnetic component of the laser field.

and all other matrix elements are zero. In our case $b_J(g_\perp - g_n)$ is about ten times larger than $a_J(g_z - g_\perp)$; therefore, the latter is negligible for a rough calculation. The effect due to these matrix elements can be taken into account by means of the second-order perturbation theory either before or after diagonalizing the 3×3 matrix obtained from (6a)–(6f).[22]

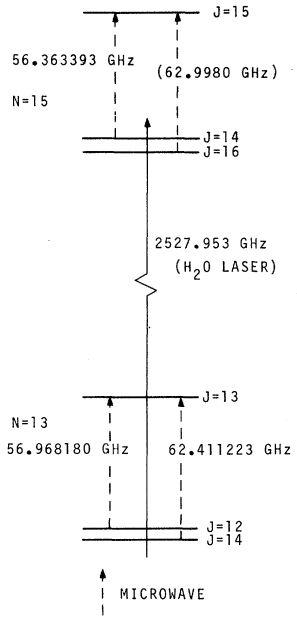

FIG. 3. The triplet levels with $N=13$ and 15. The transition frequencies within each triplet are observed in microwave spectroscopy (Refs. 11 and 12), except for $J=16\rightarrow15$.

TABLE I. Observed resonance fields and calculated perturbation energies (GHz). 119-μm parallel transitions. Perturbations in $N=15$ and 13 states are from each of the $N=J$ levels, and calculated using the g factors given in (3b). The differences between the perturbations energies of $N=15$ and 13 states are calculated using the g factors given in (3b), (3a), and (9). The accuracy in the observed field strengths is 0.5 G for lines below 8 kG, 1.0 G for lines between 8 and 12 kG, and 1.5 G for lines between 12 and 20 kG; this corresponds to about 2.5 MHz for the energy differences.

$\mathcal{B}$ (kG)		4.7793	5.1762	5.6446	6.2043	6.8818	7.7099	8.7279	9.9682	11.4386	13.0739	14.7492	16.3031	
M		−14	−13	−12	−11	−10	−9	−8	−7	−6	−5	−4	−3	Average
$N=15$		−44.144	−44.406	−44.737	−45.160	−45.711	−46.436	−47.395	−48.652	−50.238	−52.105	−54.098	−56.001	
$N=13$		−75.818	−76.081	−76.411	−76.834	−77.385	−78.109	−79.068	−80.322	−81.913	−83.776	−85.769	−87.673	
Difference	(3b)	31.674	31.674	31.674	31.674	31.674	31.673	31.673	31.670	31.675	31.671	31.671	31.672	31.673
	(3a)	31.669	31.669	31.669	31.669	31.669	31.669	31.668	31.666	31.670	31.667	31.666	31.667	31.668
	(9)	31.666	31.667	31.667	31.666	31.667	31.666	31.666	31.663	31.668	31.665	31.665	31.666	31.666

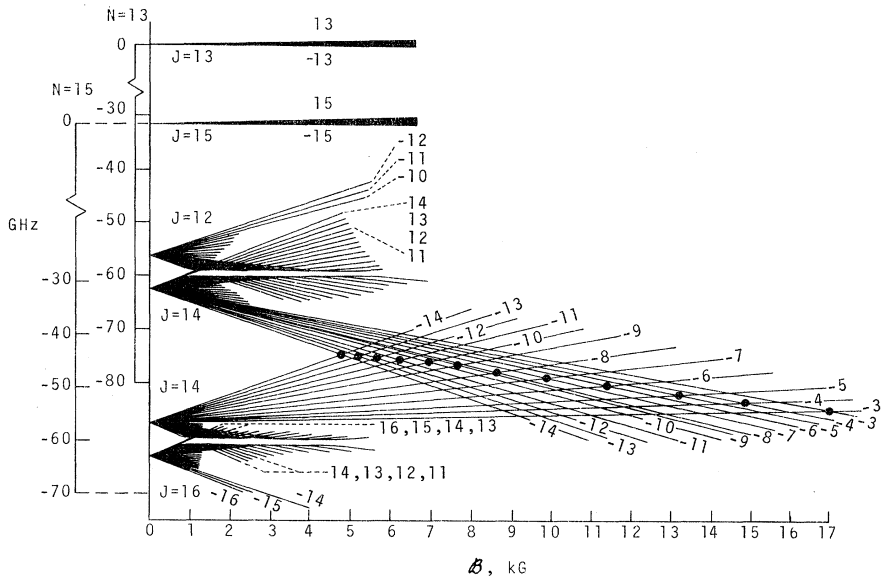

FIG. 4. A schematic energy-level diagram to illustrate the laser magnetic resonances at 119 μm. All the $N=13$ levels are shifted up by the laser frequency so that an appropriate level of $N=13$ crosses the corresponding one of $N=15$ at the resonance field of the transition.

III. EXPERIMENT

The laser-magnetic-resonance spectrometer is shown in Fig. 1. The laser oscillates between mirrors C and D and is divided into two parts with the dielectric beam splitter. The sample is in one part and the active medium of the laser is in the other. The beam splitter restricts the field of the laser to linear polarization. A valve (not shown) permits the connection of both sides for simultaneous evacuation in order to protect the beam splitter. The 0.5-mil polyethylene or polypropylene beam splitter can be rotated from the Brewster angle (about an axis perpendicular to the laser axis) to increase the coupling to the laser cavity. The entire beam-splitter assembly (including detectors) can be rotated about the laser axis in order to change the polarization of the laser with respect to the magnetic field. Detector A was used to set the laser to the center of the laser line, and detector B fed the amplifier synchronized with the modulation coil modulated at 84 Hz. A 15-in. magnet with $5\frac{1}{2}$-in. Rose shimmed pole tips was used; it permitted fields up to 23.5 kG. A modulation amplitude of about 2 G was used with an oxygen pressure of 2 Torr for recording the spectra. The linewidth of the 4779-G line was 1.2 G at a pressure of 0.9 Torr. The 11.4-kG line was nearly twice as wide as the 4.8-kG line. Higher field lines were increasingly broader due to increasing magnetic inhomogeneity and decreasing energy change per field.

The magnetic field strength at the center of the parallel and some of the perpendicular transition lines was accurately measured with an NMR gaussmeter and frequency counter. A correction was made for the difference in field strength between the NMR location and the center of the sample cell.

Standard golay cells were used as detectors. Detector B received the full laser output of a few milliwatts; no saturation of this detector was observed, even at this power level, apparently because the laser-magnetic-resonance signal was a small ac signal superposed on the steady laser output.

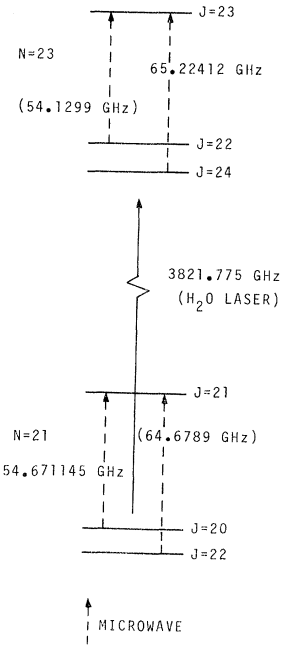

FIG. 5. The triplet levels with $N=21$ and 23. Two of the transition frequencies within each triplet are observed in microwave spectroscopy and two others are calculated (Refs. 11 and 12).

TABLE II. Observed resonance fields and calculated perturbation energies (GHz). 119-μm perpendicular transitions. Perturbation energies are from $N=J$ level, and calculated using the g factors given in (3b). The differences between the perturbation energies of $N=15$ and 13 states are calculated using the g factors given in (3b), (3a), and (9). The accuracy in the observed field strengths is about 5 in each of the last digits.

$\mathcal{B}$ (kG)		4.9345[a]	5.0056[a]	5.360	5.441	5.8639[a]	5.9591[a]	6.470	6.581	7.2097[a]	7.340	8.112	8.262	9.230
M ($N=15$)		−14	−13	−13	−12	−12	−11	−11	−10	−10	−9	−9	−8	−8
M ($N=13$)		−13	−14	−12	−13	−11	−12	−10	−11	−9	−10	−8	−9	−7
$N=15$		−43.758	−44.776	−44.01	−45.11	−44.334	−45.536	−44.76	−46.08	−45.322	−46.77	−46.09	−47.68	−47.10
$N=13$		−75.435	−76.453	−75.69	−76.79	−76.010	−77.212	−76.43	−77.75	−76.999	−78.45	−77.75	−79.35	−78.77
Difference	(3b)	31.677	31.677	31.68	31.67	31.676	31.676	31.67	31.67	31.677	31.68	31.66	31.66	31.67
	(3a)	31.673	31.673	31.68	31.67	31.673	31.671	31.67	31.67	31.673	31.68	31.66	31.66	31.66
	(9)	31.667	31.668	31.67	31.67	31.668	31.668	31.67	31.67	31.669	31.67	31.65	31.66	31.66

$\mathcal{B}$ (kG)		9.395	10.587	10.758	12.137	12.305	12.477[b]	13.820	13.960	15.460	15.565	16.825[c]	16.907	16.982
M ($N=15$)		−7	−7	−6	−6	−5		−5	−4	−4	−3	5	−3	−2
M ($N=13$)		−8	−6	−7	−5	−6		−4	−5	−3	−4	4	−2	−3
$N=15$		−48.86	−48.45	−50.35	−50.14	−52.12		−52.10	−54.05	−54.14	−55.94	−56.23	−56.05	−57.58
$N=13$		−80.52	−80.11	−82.02	−81.77	−83.77		−83.75	−85.70	−85.78	−87.58	−87.87	−87.69	−89.22
Difference	(3b)	31.66	31.66	31.67	31.63	31.65		31.65	31.65	31.64	31.64	31.64	31.65	31.64
	(3a)	31.66	31.66	31.67	31.62	31.64		31.65	31.64	31.64	31.63	31.63	31.64	31.64
	(9)	31.65	31.65	31.66	31.64	31.64		31.64	31.64	31.64	31.63	31.63	31.64	31.64

$\mathcal{B}$ (kG)		17.890[c]	18.037	18.090	18.675[c]	18.795	18.840	19.090[c]	19.120	19.140[c]	19.180
M ($N=15$)		4	−2	−1	3	−1	0	1	2	0	1
M ($N=13$)		3	−1	−2	2	0	−1	2	1	1	0
$N=15$		−57.65	−57.65	−58.81	−58.78	−58.84	−59.55	−59.78	−59.51	−59.56	−59.78
$N=13$		−89.30	−89.29	−90.45	−90.43	−90.50	−91.21	−91.44	−91.16	−91.21	−91.44
Difference	(3b)	31.65	31.64	31.64	31.65	31.66	31.66	31.66	31.65	31.65	31.65
	(3a)	31.64	31.64	31.64	31.64	31.65	31.66	31.66	31.65	31.65	31.65
	(9)	31.64	31.64	31.63	31.64	31.65	31.65	31.65	31.65	31.65	31.65

[a]Carefully measured lines.
[b]The intensity of this line is about the same as those of 12.137- and 12.305-kG lines. No explanation of this line is found.
[c]Weak lines.

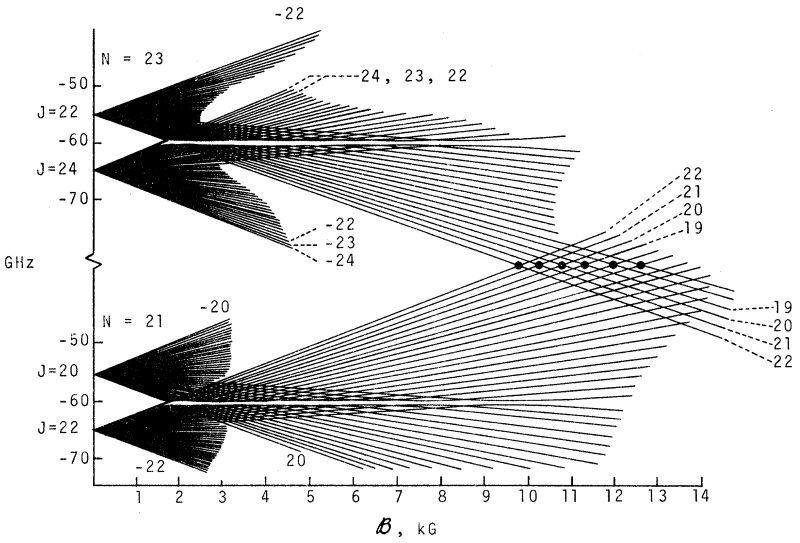

FIG. 6. A schematic energy-level diagram to illustrate the laser magnetic resonances at 78 μm. All the $N=21$ levels are shifted up by the laser frequency so that an appropriate pair of levels cross each other at the appropriate resonance fields.

IV. LASER MAGNETIC RESONANCES AT 119 μm

Figure 2 shows typical recorder traces for the resonances observed using the 119-μm line of the H_2O laser at magnetic fields between 4.5 and 16.5 kG. All magnetic fields for the parallel case, in which the magnetic component of the laser field is parallel to the external magnetic field, are measured carefully, and a few resonance magnetic fields for the perpendicular case are measured to the same accuracy. They are shown in Tables I and II. These resonances are due to the $N=13 \rightarrow 15$ transitions. The relevant zero-field energy levels are shown in Fig. 3, where the previously observed[11,12] microwave frequencies for the transitions within each triplet are also shown. Figure 4 shows the perturbations due to the external field and the observed transitions.

Taking these observed microwave frequencies for the eigenvalues of $\hat{H}$, and assuming a set of values for the g factors, we obtain a 3×3 matrix for each triplet from formulas (6a) through (6f).

The second-order effect due to the neighboring triplets is calculated from the matrix elements (7a)–(7c), and the result for the states of our interest is

$$\Delta\epsilon(15_-M) = -\Delta\epsilon(13_+M) = 0.91\mathcal{B}^2 + 0.033(\mathcal{B}M)^2 \text{ kHz}, \tag{8}$$

when $\mathcal{B}$ is in kG. For $M=-14$ and -3 this formula gives 0.17 and 0.32 MHz, respectively, at their resonance fields, and the value lies between these two values; however, the magnetic field is so high that the formula (8) is not valid. It is found that the values given by (8) are still approximately correct for the middle state of $N=15$ states, and the perturbation tends to be zero for the lowest state of $N=13$ states. For the difference between them, which is of main interest, this perturbation is therefore 0.3 MHz and almost independent of M.

Tables I and II show differences of the perturbation energies of relevant states, calculated using the existing two sets of the g factors which are given in (3a) and (3b). An extensive search to find the best values of the g factors failed to yield the required set with an accuracy higher than those claimed by Hendrie and Kusch[21] and Bauer, Kamper, and Lustig.[20] It was found that our data are sensitive to the value of g_s, but not so sensitive to those of $g_\perp$ and g_n. A much higher experimental accuracy is needed to pinpoint the values of $g_\perp$ and g_n. The "best" g values as determined by this experiment are

$$g_\perp = 2.0044 \pm 0.0008, \quad g_s = 2.0020 \pm 0.0001,$$
$$g_n = 0.000125 \pm 0.000008 . \tag{9}$$

The energy differences calculated using this set are also shown in Tables I and II. It is seen that Hendrie and Kusch's set is slightly better than Bauer, Kamper, and Lustig's set, but the best set is closer to the latter.

When we take all parallel resonances and five carefully measured perpendicular resonances, we find that average energy difference is 31.6741, 31.6693, and 31.6666 GHz, when the g factors of (3b), (3a), and (9) are taken, respectively. Taking the average of these three possible values and the observed frequency of the 119-μm H_2O laser line,[22] 2527.953 GHz, we obtain

$$\nu[(N=J=13) \rightarrow (N=J=15)] = 2496.283 \pm 0.030 \text{ GHz} \tag{10}$$

as the zero-field transition frequency.

TABLE III. Observed resonance fields and calculated perturbation energies (GHz). 78-μm parallel transitions. Perturbations are from the $N=J$ level of each triplet. The accuracy in the observed field strengths is from 3 G (for $M=22$) to 15 G for high-field lines. The average energy difference is -44.04 ± 0.03 GHz.

$\mathcal{B}$ (kG)	9.870	10.435	11.045	11.725	12.450	13.24	14.10	15.03
M	22	21	20	19	18	17	16	15
$N=23$	−80.99	−81.72	−82.52	−83.45	−84.45	−85.57	−86.83	−88.23
$N=21$	−36.96	−37.66	−38.48	−39.38	−40.42	−41.57	−42.83	−44.19
Difference	−44.03	−44.07	−44.05	−44.08	−44.03	−44.00	−44.00	−44.04

No explanation is found for the strong resonance at 12.477 kG.

V. LASER MAGNETIC RESONANCES AT 78 μm

Relatively weak resonances, listed in Table III, are observed at 78 μm with the magnetic component of the laser field parallel to the external magnetic field.

These resonances are due to the $N=21\rightarrow23$ transitions. The relevant zero-field energy levels are shown in Fig. 5, where the previously observed (and calculated)[11,12] microwave frequencies for the transitions within each triplet are also shown. Figure 6 shows the perturbation due to the external field and the transitions observed.

Since the resonances were weak, their field strengths were not measured accurately. The theoretical calculation is done in the same way as in the case of the 119-μm line, but the second-order effect due to the neighboring triplets is 0.2 MHz and is completely negligible in the present accuracy. Also the differences between the three sets of the g factors, (3a), (3b), and (9), are negligible in the present accuracy. The calculated perturbation energies which are shown in Table III are obtained by using the set (3b).

From the average of the energy differences given in Table III and the observed frequency[23] of the 78-μm line of the H_2O laser, 3821-775 GHz, we obtain

$$\nu[(N=J=21)\rightarrow(N=J=23)]=3865.81\pm0.03\ \text{GHz} \tag{11}$$

for the zero-field transition frequency.

No resonance was observed at the 79-μm line of the H_2O laser.

VI. ROTATIONAL CONSTANTS

McKnight and Gordy[13] observed $N=1\rightarrow3$ transitions. From their data one obtains

$$\nu[(N=J=1)\rightarrow(N=J=3)]=430.98528\pm0.00020\ \text{GHz}\ . \tag{12}$$

Theoretically[11,12] we expect that

$$\epsilon(N=J=3)-\epsilon(N=J=1)=10B_0'+140B_1+1720B_2\ , \tag{13a}$$

$$\epsilon(N=J=15)-\epsilon(N=J=13)=58B_0'+24\,476B_1+7\,795\,432B_2\ , \tag{13b}$$

and

$$\epsilon(N=J=23)-\epsilon(N=J=21)=90B_0'+91\,260B_1+69\,585\,480B_2\ , \tag{13c}$$

where

$$B_0'=B_0+\tfrac{2}{3}\lambda_1-\mu_1\ . \tag{14}$$

Comparing these theoretical formulas with our result of (12), (10), and (11) we obtain

$$B_0'=43.100557\pm0.000020\ \text{GHz}\ , \tag{15}$$

$$B_0=43.100518\pm0.000020\ \text{GHz}\ , \tag{16a}$$

$$B_1=-0.14496\pm0.00030\ \text{MHz}\ , \tag{16b}$$

$$B_2=-0.17\pm1.00\ \text{Hz}\ , \tag{16c}$$

for the rotational constants. The uncertainties listed are one standard deviation. We used the known values[11,12,14,15,24] of λ_1 and μ_1 in obtaining Eq. (16a) from Eq. (15).

Babcock and Herzberg[25] reported $B_0=43103.27\pm0.45$ and $B_1=-0.1472\pm0.0006$ MHz. However, recent reanalysis[26] of their data showed that $B_0=43101.38\pm0.75$ MHz and $B_1=-0.1452\pm0.0016$ MHz are more plausible values. Theoretical calculation using a plausible adiabatic potential gives[26] $B_2=-0.0011$ Hz. Our values agree with these recent ones, and also are consistent with those obtained from microwave data.[24]

ACKNOWLEDGMENT

We thank Liviu Tomutza for helping with the computer calculations.

*Work partially supported by NSF Grant No. GP-27444.

[1]H. A. Kramers, Z. Physik 53, 422 (1929).
[2]M. H. Hebb, Phys. Rev. 49, 610 (1936).
[3]R. Schlapp, Phys. Rev. 51, 342 (1937).
[4]R. Beringer, Phys. Rev. 70, 53 (1946).
[5]M. W. P. Strandberg, C. Y. Meng, and J. G. Inger-

soll, Phys. Rev. 75, 1524 (1949).
[6]J. H. Burkhalter, R. S. Anderson, W. V. Smith, and W. Gordy, Phys. Rev. 79, 651 (1950).
[7]B. V. Gokhale and M. W. P. Strandberg, Phys. Rev. 84, 844 (1951).
[8]R. S. Anderson, C. M. Johnson, and W. Gordy, Phys. Rev. 83, 1061L (1951).
[9]S. L. Miller and C. H. Townes, Phys. Rev. 90, 537 (1953).
[10]M. Mizushima and R. M. Hill, Phys. Rev. 93, 745 (1954).
[11]R. W. Zimmerer and M. Mizushima, Phys. Rev. 121, 152 (1961).
[12]B. G. West and M. Mizushima, Phys. Rev. 143, 31 (1966).
[13]J. S. McKnight and W. Gordy, Phys. Rev. Letters 21, 1787 (1968).
[14]R. Tischer, Z. Naturforsch. 22A, 1711 (1967).
[15]T. T. Wilheit Jr. and A. H. Barrett, Phys. Rev. A 1, 213 (1970).
[16]K. M. Evenson, H. P. Broida, J. S. Wells, R. J. Mahler, and M. Mizushima, Phys. Rev. Letters 21, 1038 (1968).
[17]R. Beringer and J. G. Castle, Phys. Rev. 75, 1963 (1949); 81, 82 (1951).
[18]A. Henry, Phys. Rev. 80, 396 (1950).
[19]M. Tinkham and M. W. P. Strandberg, Phys. Rev. 97, 951 (1955).
[20]K. D. Bauers, R. A. Kamper, and C. D. Lustig, Proc. Roy. Soc. (London) A251, 565 (1959).
[21]J. M. Hendrie and P. Kusch, Phys. Rev. 107, 716 (1957). Their values are slightly revised here using the new value of g_s(free) = 2.0023193154; M. Mizushima, J. Math. Phys. 12, 2216 (1971).
[22]L. Frenkel, T. Sullivan, M. A. Pollack, and T. J. Bridge, Appl. Phys. Letters 11, 344 (1967); L. O. Hocker and A. Javan, Phys. Letters 26A, 255 (1968).
[23]K. M. Evenson, J. S. Wells, L. M. Matarrese, and L. B. Elwell, Appl. Phys. Letters 16, 159 (1970).
[24]W. M. Welch and M. Mizushima, Phys. Rev. A 5, 2692 (1972).
[25]H. D. Babcock and L. Herzberg, Astrophys. J. 108, 167 (1948).
[26]D. L. Albritton, W. J. Harrop, A. L. Schmeltekopt, and R. N. Zare (unpublished).

PHYSICAL REVIEW A VOLUME 6, NUMBER 5 NOVEMBER 1972

Entropy Changes in the Steady State far from Equilibrium

Rolf Landauer and James W. F. Woo
IBM Thomas J. Watson Research Center, Yorktown Heights, New York 10598
(Received 14 June 1972)

A relationship $dS = dQ/T$ is derived for slow changes in a steady-state system far from equilibrium. Systems consisting of one conservative degree of freedom, coupled to a dissipative nonequilibrium system without energy storage are considered. The entropy S is defined in the conventional statistical mechanical sense by an integral $-k\int \rho \ln\rho\, dq$ over the conservative degree of freedom. The fluctuations are assumed to be narrow and the temperature T is the noise temperature, i.e., the temperature characterizing the intensity of the fluctuations in stored energy. $-dQ$ is the energy given up to the reservoir to the extent that it exceeds that predicted for steady-state losses on the basis of the macroscopic equations. Generalizations to the case of two or more degrees of freedom are successful only in special cases. These include the case where one degree of freedom adjusts rapidly compared to the other. It also includes cases where the different degrees of freedom see the same noise temperature.

INTRODUCTION

There has been increasing interest in the development of analogies between some excited dissipative steady-state systems and thermal-equilibrium systems.[1-6] Thus far, the emphasis has been on the existence of a simple exponential form for the distribution function of these nonequilibrium systems. For instance, in the case of a laser,[2,6] the steady-state distribution function is most naturally expressed in the form $\rho = e^{-F}$. The exponent F is a function of the pumping strength and the radiated internal field and is analogous to the free energy in the equilibrium system, although F may have no obvious connection to energies actually stored in the system. Near threshold, F behaves like the Ginzburg–Landau free energy of a system near a second-order phase transition with the pump intensity taking the place of the temperature and the internal field taking the place of the order parameter. The analogy therefore exists on a formal level. That is, the distribution functions have the same form and fluctuations of analogous quantities (internal electric field corresponding to order parameter) have similar behavior. Thus far, the analogy has not been carried to a thermodynamic level.

In this paper, we attempt to give these analogies a more thermodynamic significance. In particular, we will generalize the relation $T\,dS = dQ$ to some simple nonequilibrium systems. Here dS is the change in entropy between two steady states. The